MITIGATING FORCE OSCILLATIONS IN A WAVE ENERGY CONVERTER USING CONTROL BARRIER FUNCTIONS

Mathias Marley

Department of Marine Technology

Norwegian University of Science and Technology

Trondheim, Norway

Email: mathias.marley@ntnu.no

Roger Skjetne

Department of Marine Technology

Norwegian University of Science and Technology

Trondheim, Norway

Email: roger.skjetne@ntnu.no

ABSTRACT

Control barrier functions (CBFs) is a novel feedback control strategy for enforcing safety constraints of mechanical systems. An appealing feature of the CBF method is that the safety objective is defined and enforced independent of the underlying control objective. This enables the merging of CBF-based control with any existing nominal control strategy, by imposing the safety objective as input constraints in a convex optimization problem. CBFs are gaining popularity in the robotics community, in particular for motion control of autonomous vehicles. Yet, limited use of CBFs for mechanical devices such as wave energy converters (WECs) are reported in literature. This paper motivates the use of CBF-based control for constraint satisfaction of WECs, using the Bolt Lifesaver point absorber WEC developed by Fred. Olsen Ltd. as a case study. During initial sea trials of Bolt Lifesaver, large force oscillations were observed in the power take-off unit. The source of oscillations was identified as sudden saturation of the actuator force provided by the generator. Mitigating the undesired response using conventional feedback control is non-trivial, since any such control strategy will attempt to cancel inertia forces, resulting in a reduced stability margin of the system. Using higher order CBF theory, we design a robust controller that ensures safe operation of the device, while minimally interfering with the existing control law optimized for power output. The theoretical results are verified by numerical simulations.

FIGURE 1. Bolt Lifesaver pictured outside Falmouth Bay, England, where she was deployed in 2012. Courtesy Fred. Olsen Ltd.

INTRODUCTION

The control problem for a wave energy converter (WEC) is to maximize power production while maintaining structural integrity of the device [1]. Designing a controller with satisfactory performance in both regards is often challenging. Of the more popular solutions to the WEC control problem in recent years is model predictive control (MPC) and MPC-like algorithms [2], as evidenced by the contributions to the *wave energy converter control competition* [3]. An advantage of MPC-type controllers is the ability to handle safety constraints, such as force or displacement limitations. The disadvantage of MPC lies in the complexity of the control system, and in general the non-convexity of the

numerical optimization problem [1]. For this reason, feedback controllers also remain popular, although they struggle with hard safety constraints [1].

Control barrier functions (CBFs) [4] is a novel feedback control strategy that is gaining popularity in the robotics community, with successful application to areas such as obstacle avoidance of autonomous vehicles [5–10], adaptive cruise control and lane keeping [11], robotic grasping [12], and bipedal walking robots [13–15]. Yet, limited use of CBFs applied to mechanical devices such as WECS are reported in literature. An appealing feature of the CBF method is that the safety objective is defined and enforced independent of the underlying control objective. To be precise, the CBF design requires no knowledge of the underlying control objective. CBFs are used to define a state-dependent set of admissible control inputs that maintains the system in a safe state. The admissible input set may then be posed as input constraints in a convex optimization problem that finds a safe input that minimally interferes with the nominal control objective. The resulting optimization problem has equally many decision variables as control inputs, which for most applications means it can be solved in real-time. Moreover, in the case of a single safety constraint, the optimization problem admits a closed-formed solution, avoiding the need for numerical optimization altogether. Since the admissible input set is a function of the current system states, as opposed to predicted future system states, CBFs may be used to solve both the safety objective and nominal objective using only feedback control, unless the two objectives are directly in conflict - in which case the safety objective takes presedence.

In this paper, we propose a CBF-based controller that mitigates force oscillations in the Bolt Lifesaver WEC developed by Fred. Olsen Ltd. (see [17] and references therein), depicted in Figure 1. A conceptual sketch of the device is shown in Figure 2. The device consists of a heaving body (referred to as floater) and a power take-off (PTO) unit. The PTO unit consists of a taut mooring line mounted on a drum, connected to a generator through a gearbox. Bolt Lifesaver has undergone pre-commercial sea trials outside Falmouth Bay, England, before relocation to Hawaii. During the sea trials, large force oscillations were observed in the mooring line, see Figure 3. The source of oscillations was identified as transient inertia loads in the PTO unit due to sudden saturation of the actuator force provided by the generator. Various control strategies to mitigate the undesired response were explored in [16]. Mitigating the undesired response using conventional feedback control is non-trivial, since any such control strategy will attempt to cancel inertia forces, resulting in a reduced stability margin of the system [16]. Using higher order CBF theory, we design a robust controller that ensures safe operation of the device, while minimally interfering with the nominal control law.
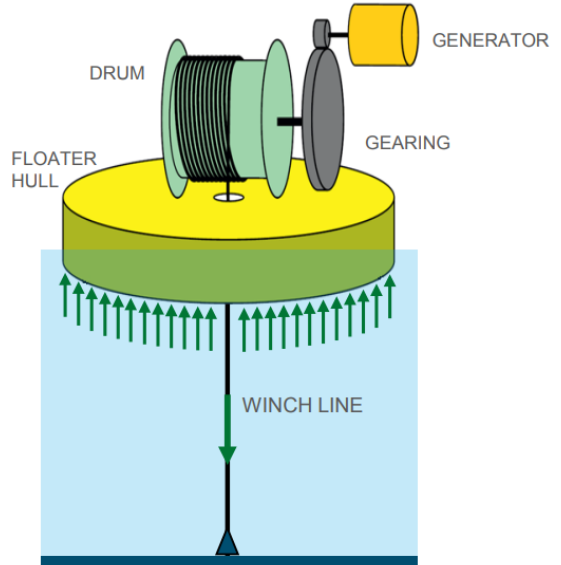

FIGURE 2. Illustration of the Bolt WEC concept. The *winch line* is in this paper referred to as *mooring line*. Courtesy Fred. Olsen Ltd.
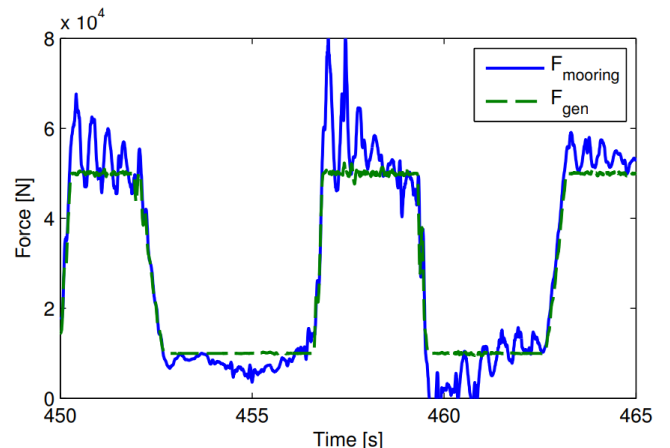

FIGURE 3. Characteristic force oscillations recorded during testing in rough sea [16]. $F_{mooring}$ is the tension in the mooring line, while F_{gen} is the actuator force provided by the generator.

Notation and preliminaries. $\mathbb{R}$ is the set of real numbers and $\mathbb{R}^n$ is the n-dimensional Euclidean space. The Lie derivative of a scalar function $B : \mathbb{R}^n \to \mathbb{R}$ along a vector field $f : \mathbb{R}^n \to \mathbb{R}^n$ is denoted $L_f B(x) := \nabla B(x)^\top f(x)$, where ∇ is the gradient operator. $F : \mathbb{R}^n \rightrightarrows \mathbb{R}^m$ denotes that F is a set-valued mapping from $\mathbb{R}^n$ to $\mathbb{R}^m$. The time derivative of x is denoted $\dot{x}$.

Definition 1. *A continuous function* $\alpha : \mathbb{R} \to \mathbb{R}$ *is an extended class$-\mathscr{K}$ function if it is strictly increasing and* $\alpha(0) = 0$.

2

CONTROL BARRIER FUNCTIONS

CBFs ensure safety for affine control systems of the form

$$\dot{x} = f(x) + g(x)u, \tag{1}$$

with state $x \in \mathbb{R}^n$ and input $u \in \mathbb{R}^m$. Let $B_1 : \mathbb{R}^n \to \mathbb{R}$ be a continuously differentiable function that defines a safe set

$$K_1 := \{x \in \mathbb{R}^n : B_1(x) \leq 0\}. \tag{2}$$

The evolution of B_1 along the solutions of system (1) is given by

$$\dot{B}_1 = \nabla B_1(x)^\top \dot{x} = L_f B_1(x) + L_g B_1(x)u, \tag{3}$$

where $L_f B_1$ and $L_g B_1$ are the Lie derivatives of B_1 along f and g, respectively. The key idea behind CBFs is to control the evolution of B_1 to maintain the system states inside the set K_1. If $L_g B_1(x) \neq 0$, this is achieved by selecting u such that

$$L_f B_1(x) + L_g B_1(x)u \leq -\alpha_1(B_1(x)), \tag{4}$$

where $\alpha_1 : \mathbb{R} \to \mathbb{R}$ is an extended class-$\mathscr{K}$ function. Observe that when the inequality (4) is satisfied, $\dot{B}_1$ must be negative if $B_1(x) > 0$, while $\dot{B}_1$ may be positive if $B_1(x) < 0$.

If $L_g B_1(x) = 0$, that is, if the control input does not appear in the first derivative of B_1, the safety constraint may be enforced by using higher order CBFs (HOCBFs) [18]. B_1 is an HOCBF candidate of order r if

$$L_g L_f^{r-i} B_1(x) = 0, \quad \forall x \in \mathbb{R}^n, \ \forall i \geq 2, \tag{5}$$
$$L_g L_f^{r-1} B_1(x) \neq 0, \quad \text{for some } x \in \mathbb{R}^n. \tag{6}$$

Given an HOCBF candidate of order r, we recursively define a series of functions $B_i : \mathbb{R}^n \to \mathbb{R}$, for $i \in \{2, ..., r\}$, as

$$B_i(x) := L_f B_{i-1}(x) + \alpha_{i-1}(B_{i-1}(x)), \tag{7}$$

where $\alpha_{i-1} : \mathbb{R} \to \mathbb{R}$ are sufficiently differentiable extended class$-\mathscr{K}$ functions. Define the sets

$$K_i := \{x \in \mathbb{R}^n : B_i(x) \leq 0\}, \quad K := \bigcap_{i=1}^{r} K_i. \tag{8}$$

Definition 2 (Adapted from [10, Definition 7]). *Let B_1 be an HOCBF candidate of order r that defines the set K_1 in (2). Let B_i, for $i \in \{2, ..., r\}$ be defined in (7), and let K be defined in (8). B_1 is an HOCBF of order r if there exists an extended class$-\mathscr{K}$ function α_r and an open set $\mathscr{U}$ containing K such that*

$$\inf_{u \in U} \left[L_f B_r(x) + L_g B_r(x)u \right] \leq -\alpha_r(B_r(x)), \quad \forall x \in \mathscr{U}. \tag{9}$$

Admissible input set

B_r and α_r define an admissible input set $U_B : \mathbb{R}^n \rightrightarrows \mathbb{R}^m$,

$$U_B(x) := \{u \in \mathbb{R}^m : L_f B_r(x) + L_g B_r(x)u \leq -\alpha_r(B_r(x))\}. \tag{10}$$

For each x, $U_B(x)$ is the set of control inputs such that $\dot{B}_r \leq -\alpha_r(B_r(x))$ is satisfied. Definition 2 above states that B_1 is an HOCBF if $U_B(x)$ is nonempty for all x on a neighborhood of the intersection $K = K_1 \cap \cdots \cap K_r$. Roughly speaking, a set K is forward invariant if all solutions starting in K remain in K for all future time. For any $u \in U_B(x)$, B_r is non-increasing on the boundary of K_r and strictly decreasing outside K_r, which implies forward invariance and local attractivity of K_r. Since

$$\dot{B}_{r-1} = L_f B_{r-1}(x) = -\alpha_{r-1}(B_{r-1}(x)) + B_r(x), \tag{11}$$

and $x \in K_r \implies B_r(x) \leq 0$, solutions cannot leave K_{r-1} while inside the set K_r. Recursively applying similar arguments, we arrive at the conclusion that any input $u \in U_B(x)$ renders the intersection K forward invariant. Since $K \subset K_1$, solutions starting in K will then remain in the safe set K_1 defined by B_1.

Theorem 1 (Adapted from [10, Theorem 8]). *If B_1 is an HOCBF for system (1), then K is forward invariant for the system*

$$\dot{x} \in \{f(x) + g(x)u : u \in U_B(x)\}. \tag{12}$$

Proof. See [10, Theorem 8]. $\qquad\square$

CBFs are robust towards bounded disturbances, in the sense that solutions of the disturbed system

$$\dot{x} \in \{f(x) + g(x)u + w : u \in U_B(x)\}, \tag{13}$$

starting in K, remain close to K, for sufficiently small disturbances w. This result was shown in [19], in the context of first order CBFs, while the extension to HOCBFs follows from the results of [20].

Safety-critical controller

A CBF may be combined with any nominal control $\kappa : \mathbb{R}^n \to \mathbb{R}^m$, by solving an optimization problem [11],

$$\kappa_B(x) := \arg\min_{u \in U_B(x)} [u - \kappa(x)]^\top P[u - \kappa(x)], \tag{14}$$

where $P \in \mathbb{R}^{m \times m}$ is a diagonal positive definite matrix. In the case of multiple safety-constraints enforced by individual CBFs, e.g. both upper and lower bounds on allowed displacements, U_B becomes the intersection of the admissible input sets defined by

the respective associated CBFs. For a single safety constraint, and assuming $L_g B_1(x) \neq 0, \forall x \in \mathbb{R}^n$, the control law (14) admits a closed-form solution given by [10]

$$
\kappa_B(x) = \begin{cases} \kappa(x), & \kappa(x) \in U_B(x) \\ \kappa(x) - \dfrac{a(x)b(x)^\top}{b(x)b(x)^\top} & \kappa(x) \notin U_B(x) \end{cases}
$$
$$
a(x) := L_f B(x) + L_g B(x)\kappa(x) + \alpha(B(x)),
$$
$$
b(x) := L_g B(x) P^{-0.5}. \tag{15}
$$

x_1

m_1

u
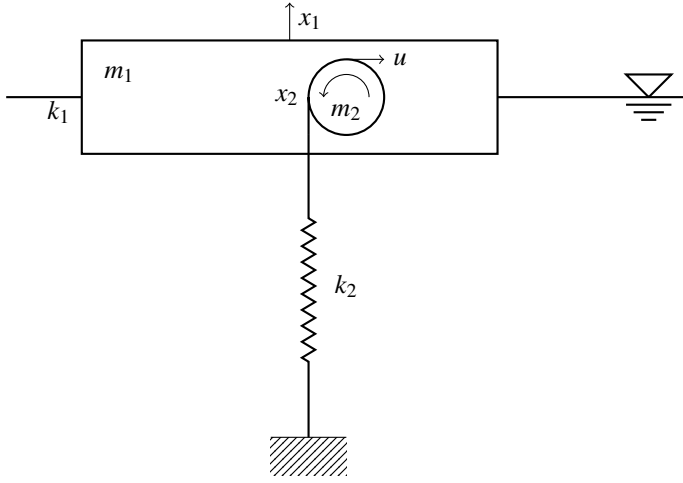
x_2 m_2

k_1

k_2

FIGURE 4. Illustration of control design model of Bolt Lifesaver.

CONTROL SYSTEM DESIGN FOR BOLT WEC

In this section, we design a safety-critical controller for Bolt Lifesaver. To this end, we require a reduced order model of low complexity, that qualitatively captures the WEC dynamics. Inevitably, there will be significant modeling error. From a control systems perspective, the modeling error is viewed as unknown disturbances, and we rely on the robustness properties of CBFs for disturbance rejection. We make use of the two degree of freedom control design model (CDM) proposed in [16], illustrated in Figure 4. Let x_1 denote the heave displacement of the floater, defined positive upwards. The heave dynamics are modeled by

$$
m_1 \ddot{x}_1 + d_1 \dot{x}_1 + k_1 x_1 = F_w - F_m, \tag{16}
$$

where $m_1 > 0$ is the total inertia (including hydrodynamic added mass), $d_1 > 0$ is a linearized damping coefficient, while k_1 is the hydrostatic stiffness. The wave force F_w is defined positive upwards, while the mooring line force F_m is defined positive under

tension. Define $x_2 := L - L_0$, where L is the unstretched mooring line length and L_0 is the distance from drum to anchor point when $x_1 = 0$. Neglecting line dynamics, the mooring line force becomes

$$
F_m = \begin{cases} k_2(x_1 - x_2) & x_1 \geq x_2 \\ 0 & x_1 \leq x_2 \end{cases}, \tag{17}
$$

where k_2 is the axial stiffness under tension, assumed constant. The dynamic relation between mooring force and generator force F_g is given by

$$
m_2 \ddot{x}_2 + d_2 \dot{x}_2 = F_m - F_g, \tag{18}
$$

where $m_2 > 0$ is the combined inertia of the drum and gearbox in the linear coordinate system, and $d_2 > 0$ is an equivalent friction coefficient. Defining $x_3 := \dot{x}_1$ and $x_4 := \dot{x}_2$, we obtain the system

$$
\dot{x} = f(x) + g(x)u + h(x)w, \tag{19}
$$

with control input $u := F_g$, disturbance $w := F_w$, and

$$
f(x) := \begin{bmatrix} x_3 \\ x_4 \\ (-d_1 x_3 - k_1 x_1 - k_2(x_1 - x_2))/m_1 \\ (-d_2 x_4 + k_2(x_1 - x_2))/m_2 \end{bmatrix},
$$
$$
g(x) := \begin{bmatrix} 0 \\ 0 \\ 0 \\ 1/m_2 \end{bmatrix}, \quad h(x) := \begin{bmatrix} 0 \\ 0 \\ 1/m_1 \\ 0 \end{bmatrix}. \tag{20}
$$

Note that the system (19), with f, g and h defined in (20), can be stated as a linear time-invariant system $\dot{x} = Ax + Bu + Ew$. System (19) is valid for positive mooring forces. Representative parameters for Bolt Lifesaver are given in Table 1. The CDM admits two coupled eigenmodes with undamped periods $T_{n_1} = 2.7$s and $T_{n_2} = 0.48$s. The force oscillations observed during sea trials correspond to T_{n_2}, and is mainly associated with oscillations of the drum and gearbox.

Nominal control

Energy is extracted from the waves when the rope velocity is positive, i.e. when $x_4 > 0$. When $x_4 < 0$, energy is spent on reeling in the mooring line. Net power extraction is achieved by increasing the mooring line tension F_m for positive velocities, and reducing the tension for negative velocities. To maintain

TABLE 1. Model parameters

Description	Symbol	Value	Unit
Floater mass	m_1	221	tonnes
Hydrostatic stiffness	k_1	1225	kN/m
Hydrodynamic damping	d_1	5	kN/(m/s)
Lumped PTO inertia	m_2	3	tonnes
Mooring line stiffness	k_2	500	kN/m
PTO friction coefficient	d_2	0.5	kN/(m/s)

structural integrity, F_m should be kept within $[F_{min}, F_{max}]$, with $F_{max} > F_{min} > 0$ to avoid slack in the mooring line. The control law used on Bolt Lifesaver during pre-commercial testing is given by

$$u = \kappa_0(x) := \begin{cases} F_{min} & x_4 \leq 0, \\ F_{min} + bx_4, & 0 \leq x_4 \leq (F_{max} - F_{min})/b, \\ F_{max} & x_4 \geq (F_{max} - F_{min})/b \end{cases} \quad (21)$$

where $b > 0$ is the damping coefficient tuned to maximize power extraction. The control law κ_0 is a special case of the passive converter [21]. The nominal control strategy results in large force oscillations in F_m whenever the generator force saturates. Mitigating the force oscillations using a reference filter and proportional-derivative feedback control was explored in [16].

We emphasize that F_{min} and F_{max} above include a safety margin with respect to the true structural capacity limits of the device. In control system design, they are viewed as tuning parameters.

CBF design

An elegant alternative solution for mitigating force oscillations is obtained using CBF theory. We first assign $u = \kappa_0(x) + \tilde{u}$, where $\tilde{u}$ is a perturbation in the control law used to maintain $F_m \in [F_{min}, F_{max}]$. From this we define the system

$$\dot{x} = f_0(x) + g(x)\tilde{u} + h(x)w, \quad f_0(x) := f(x) + g(x)\kappa_0(x). \quad (22)$$

We use two second order CBFs to enforce $F_m \geq F_{min}$ and $F_m \leq F_{max}$, given by

$$B_{l1}(x) := F_{min} - k_2(x_1 - x_2), \quad (23)$$
$$B_{u1}(x) := k_2(x_1 - x_2) - F_{max}, \quad (24)$$

where the subscripts l and u denote lower and upper, respectively. B_{l1} and B_{u1} define the sets

$$K_{i1} := \{x : B_{i1}(x) \leq 0\}, \quad i \in \{l, u\}, \quad K_1 := K_{l1} \cap K_{u1}. \quad (25)$$

Since $x \in K_1 \implies F_m \in [F_{min}, F_{max}]$, safety is achieved by rendering K_1 forward invariant. Noting that $L_g B_{i1}(x) = L_h B_{i1}(x) = 0$, we select an inverse time constant $\gamma_1 > 0$, and define

$$B_{i2}(x) := L_{f_0} B_{i1}(x) + \gamma_1 B_{i1}(x), \quad i \in \{l, u\}, \quad (26)$$
$$K_{i2} := \{x : B_{i2}(x) \leq 0\}, \quad i \in \{l, u\}, \quad K_2 := K_{l2} \cap K_{u2}. \quad (27)$$

The input $\tilde{u}$ enters the system through x_4. We verify that, given any value of x_1, x_2, and x_3, there exists x_4, such that $x \in K_2$. Since

$$x \in K_{l2} \implies k_2 x_4 \leq k_2 x_3 + \gamma_1 k_2(x_1 - x_2) - \gamma_1 F_{min}, \quad (28)$$
$$x \in K_{u2} \implies k_2 x_4 \geq k_2 x_3 + \gamma_1 k_2(x_1 - x_2) - \gamma_1 F_{max}, \quad (29)$$

and $F_{max} > F_{min}$, this is indeed true. From this, it follows directly that the intersection of K_1 and K_2 is nonempty. Differentiating B_{l2} and B_{u2} along the solutions of (22), we obtain, for $i \in \{l, u\}$,

$$\dot{B}_{i2}(x, \tilde{u}, w) = L_{f_0} B_{i2}(x) + L_g B_{i2}(x)\tilde{u} + L_h B_{i2}(x)w. \quad (30)$$

At this point, we assume the disturbance w is known, and select an inverse time constant $\gamma_2 > 0$ to obtain the admissible input set $U_B(x, w) := U_l(x, w) \cap U_u(x, w)$, where U_l and U_u are given by

$$U_i(x, w) := \{\tilde{u} \in \mathbb{R} : \dot{B}_{i2}(x, \tilde{u}, w) \leq -\gamma_2 B_{i2}(x)\}, \, i \in \{l, u\}. \quad (31)$$

Since we are considering a single input system, the safety-critical controller (14) becomes

$$\tilde{u} = \tilde{\kappa}(x, w) := \begin{cases} 0, & 0 \in U_B(x, w), \\ \partial U_i(x, w), & 0 \notin U_i(x, w), \, i \in \{l, u\}, \end{cases} \quad (32)$$

where $\partial U_i(x, w)$ is the boundary of $U_i(x, w)$,

$$\partial U_i(x) = \frac{-\gamma_2 B_{i2}(x) - L_{f_0} B_{i2}(x) - L_h B_{i2}(x)w}{L_g B_{i2}(x)}. \quad (33)$$

NUMERICAL SIMULATIONS

A small simulation study is performed on the CDM, with the wave disturbance emulating an irregular sea state corresponding to a peak excitation period of 10s. Since the CDM does not include an explicit transfer function from wave elevation to wave excitation, the sea state is not further specified. The purpose of the simulations are to verify the theoretical contributions presented above, and motivate the use of CBF-based control strategies. Evaluating the controller performance on higher-fidelity models is beyond the scope of this paper. Control system parameters are given in Table 2.

5

TABLE 2. Control system parameters

Description	Symbol	Value	Unit
Minimum mooring force	F_{min}	10	kN
Maximum mooring force	F_{max}	100	kN
Damping coefficient	b	300	kN/(m/s)
Inverse time constant	γ_1	10	1/s
Inverse time constant	γ_2	20	1/s

Implementation of the CBF controller

Since w is unknown, it is not possible to implement the controller $\tilde{u} = \tilde{\kappa}(x, w)$. A tempting option is to simply disregard w, by assigning $\tilde{u} = \tilde{\kappa}(x, 0)$. A better option results from recognizing that the floater dynamics are significantly slower than the PTO dynamics. This, together with the fact that w is a slowly varying process relative to the PTO dynamics, allows us to make the quasistatic assumption $\dot{x}_3 \approx 0$ in the implementation of the safety-critical controller. This is equivalent to assigning $\tilde{u} = \tilde{\kappa}(x, \phi(x))$, with $\phi(x) := -d_1 x_3 - k_1 x_1 - k_2(x_1 - x_2)$.
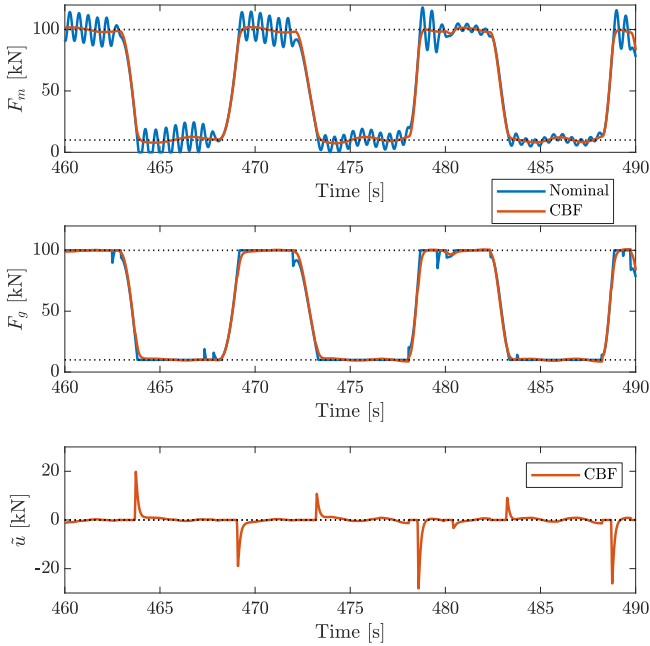

FIGURE 5. Mooring line force F_m (top) and generator force F_g (mid) for a representative time period in an irregular sea state, using only the nominal controller (blue) and the CBF-enhanced controller (red). The constraints F_{min} and F_{max} are indicated by dotted lines. Bottom plot shows the controller perturbation term $\tilde{u}$ for the CBF controller.

Results

The CBF-enhanced controller is compared to the nominal control law, where the CBF controller is implemented under the assumption $\dot{x}_3 \approx 0$. Representative mooring line response and corresponding generator force is shown in Figure 5, with a closer view in Figure 6. The CBF controller virtually eliminates the high-frequent oscillations, as desired. We say that the CBF controller is active when the controller perturbation term $\tilde{u}$ is non-zero. When the CBF controller is active, the control system seeks to exponentially stabilize $F_m = F_{min}$ or $F_m = F_{max}$.

For both controllers, the mooring force also contains an oscillatory component with frequency corresponding to the natural period of the floater, as shown in Figure 6. In the case of the CBF-based controller, this is a result of the assumption $\dot{x}_3 \approx 0$, meaning that inertial loads of the floater are not accounted for in the control law. Yet, the mooring line force remains acceptably close to the set $[F_{min}, F_{max}]$.

Discussion

The main performance benefit of the CBF controller is the ability to mitigate high-frequent PTO oscillations, which is important for reducing fatigue loads on the device. This result is expected to hold also if the controller is implemented on the physical device. Due to sufficient separation between PTO and floater eigenperiods, the controller is expected robust towards uncertainty in hydrodynamic added mass. The authors foresee two main challenges that need to be solved before implementing the CBF controller: 1) obtaining real-time estimates of the floater heave position and velocity, 2) obtaining a good estimate of the mooring line stiffness. A promising solution for solving item 1 is using the Kalman filter proposed in [16]. Item 2 may be solved by recognizing that the time-averaged mooring line force and generator force are approximately equal. This fact can be utilized in a learning algorithm or adaptive algorithm that estimates the mooring line stiffness in real time.

CONCLUDING REMARKS

This paper motivates the use of CBF-based control for WECs and similar mechanical devices, considering the Bolt Lifesaver as a case study. The resulting feedback controller is appealing in its simplicity, robust towards disturbances and maintains structural integrity of the device. The performance of the control system is illustrated by numerical simulations on the CDM. Further numerical simulation studies on higher-fidelity models of the WEC are needed to fully verify the efficacy of the control system.
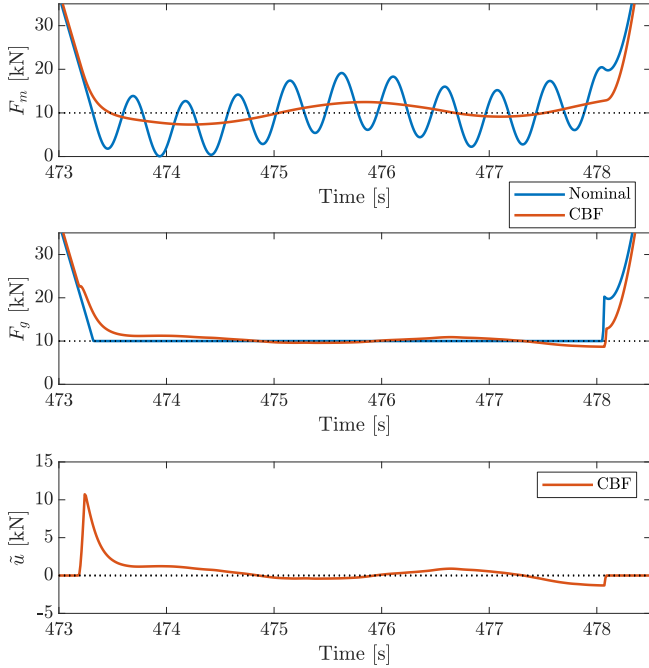
FIGURE 6. Closer view of a short time period from Figure 5. The nominal control has sudden saturation of F_g, and then maintains $F_g \equiv F_{min}$ until the rope velocity becomes positive. The CBF controller uses the perturbation term $\tilde{u}$ to exponentially stabilize $F_m = F_{min}$.

REFERENCES

[1] Ringwood, J. V., 2020. "Wave energy control: Status and perspectives 2020". *IFAC-PapersOnLine,* **53**(2), pp. 12271–12282.

[2] Faedo, N., Olaya, S., and Ringwood, J. V., 2017. "Optimal control, MPC and MPC-like algorithms for wave energy systems: An overview". *IFAC Journal of Systems and Control,* **1**, pp. 37–56.

[3] Ringwood, J., Ferri, F., Tom, N., Ruehl, K., Faedo, N., Bacelli, G., Yu, Y. H., and Coe, R. G., 2019. "The wave energy converter control competition: Overview". In Proc. Int. Conf. on Offshore Mechanics and Arctic Engineering.

[4] Ames, A. D., Coogan, S., Egerstedt, M., Notomista, G., Sreenath, K., and Tabuada, P., 2019. "Control barrier functions: Theory and applications". In Proc. European Control Conference, pp. 3420–3431.

[5] Borrmann, U., Wang, L., Ames, A. D., and Egerstedt, M., 2015. "Control barrier certificates for safe swarm behavior". *IFAC-PapersOnLine,* **48**(27), pp. 68–73.

[6] Emam, Y., Glotfelter, P., and Egerstedt, M., 2019. "Robust barrier functions for a fully autonomous, remotely accessible swarm-robotics testbed". In Proc. IEEE Conf. Decision and Control, pp. 3984–3990.

[7] Thyri, E. H., Basso, E. A., Breivik, M., Pettersen, K. Y., Skjetne, R., and Lekkas, A. M., 2020. "Reactive collision avoidance for ASVs based on control barrier functions". In Proc. IEEE Conf. Control Technology & Applications.

[8] Basso, E. A., Thyri, E. H., Pettersen, K. Y., Breivik, M., and Skjetne, R., 2020. "Safety-critical control of autonomous surface vehicles in the presence of ocean currents". In Proc. IEEE Conf. Control Technology & Applications.

[9] Marley, M., Skjetne, R., and Teel, A. R., 2021. "Synergistic control barrier functions with application to obstacle avoidance for nonholonomic vehicles". In Proc. American Control Conf., pp. 242–248.

[10] Marley, M., Skjetne, R., Basso, E. A., and Teel, A. R., 2021. "Maneuvering with safety guarantees using control barrier functions". *IFAC-PapersOnline,* **54**(16), pp. 370–377.

[11] Ames, A. D., Xu, X., Grizzle, J. W., and Tabuada, P., 2017. "Control barrier function based quadratic programs for safety critical systems". *IEEE Transactions on Automatic Control,* **62**(8), pp. 3861–3876.

[12] Shaw Cortez, W., Oetomo, D., Manzie, C., and Choong, P., 2021. "Control barrier functions for mechanical systems: Theory and application to robotic grasping". *IEEE Trans. on Control Systems Technology,* **29**(2), pp. 530–545.

[13] Hsu, S. C., Xu, X., and Ames, A. D., 2015. "Control barrier function based quadratic programs with application to bipedal robotic walking". In Proc. American Control Conf., pp. 4542–4548.

[14] Nguyen, Q., and Sreenath, K., 2021. "Robust safety-critical control for dynamic robotics". *IEEE Transactions on Automatic Control,* **9286**(c), pp. 1–16.

[15] Nguyen, Q., Hereid, A., Grizzle, J. W., Ames, A. D., and Sreenath, K., 2016. "3D dynamic walking on stepping stones with control barrier functions". In Proc. IEEE Conf. Decision and Control, pp. 827–834.

[16] Marley, M., 2014. *Modelling and robust control of production force of a wave energy converter.* Master thesis, Norwegian University of Science and Technology.

[17] Sjolte, J., 2014. "Marine renewable energy conversion: Grid and off-grid modeling, design and operation". Phd thesis, Norwegian University of Science and Technology.

[18] Xiao, W., and Belta, C., 2019. "Control barrier functions for systems with high relative degree". In Proc. IEEE Conf. Decision and Control, pp. 474–479.

[19] Xu, X., Tabuada, P., Grizzle, J. W., and Ames, A. D., 2015. "Robustness of control barrier functions for safety critical control". *IFAC-PapersOnLine,* **48**(27), pp. 54–61.

[20] Tan, X., Cortez, W. S., and Dimarogonas, D. V., 2021. "High-order barrier functions : Robustness , safety and performance-critical control". *Accepted for publication in Transactions on Automatic Control,* **PP**.

[21] Hals, J., 2010. "Modelling and phase control of wave-energy converters". Phd thesis, Norwegian University of Science and Technology.